Adaptive Network Resource Optimization for Heterogeneous VLC/RF Wireless Networks

Weihua Wu, Fen Zhou, *Senior Member, IEEE*, and Qinghai Yang

***Abstract*— Deploying a radio frequency (RF) access point (AP) to the visible light communication (VLC) system is a promising strategy to overcome the VLC's limitations, such as limited coverage, strictly line-of-sight transmission, and mobility robustness, etc. In this paper, we focus on the energy-aware design of network selection and resource allocation for a heterogeneous network combining with RF and VLC APs. For adapting to different timescale network states and stochastic data arrival, we propose an on-line two-timescale adaptive network resource optimization (ANRO) framework by employing the Lyapunov optimization technique. At the large timescale, we first develop a closed-form solution for the subproblem of network selection for user equipment. Second, we design a cost-effective and easy-to-realize algorithm for VLC's joint transmission scheduling and power control subproblem, which is a nonconvex optimization. While at the small timescale, we obtain the optimal solution for RF's joint resource block and power allocation subproblem, which is proven a mixed integer nonlinear optimization. Simulation results demonstrate that the ANRO can achieve a tradeoff between network power consumption and delay. Furthermore, it not only can stabilize the network but also can significantly reduce the energy consumption compared with other existing schemes.**

***Index Terms*— Visible light communication, network selection, resource allocation, heterogeneous network.**

I. INTRODUCTION

TO CARRY the massive media applications effectively, the community of 5G has expanded its horizon to the visible light communication (VLC) [1]. By switching at an imperceptible rate of human eye, the light emitting diodes (LED) of VLC can be used for communication where the data is encoded in the emitting light in various ways. With deploying a photodetector (PD), the user equipment (UE) can receive the modulated signals and decode the data. Hence, the LEDs can provide both illumination and communication. Although the VLC system can provide high data rate, its performance will degrade sharply in the absence of line-of-sight (LOS) transmission between VLC access point (AP) and UE. On the contrary, the radio frequency (RF) system can provide a wide range of coverage even in the absence of LOS transmission. Hence, the integration of VLC and RF in a heterogeneous wireless network (HetNet) is receiving a lot of attentions in recent years [2].

Despite that the HetNet can overcome the VLC's limitations, such as limited coverage, heavy dependence on LOS transmission and mobility robustness, *etc*, there are still many research challenges remained to be addressed for the resource optimization. First of all, different types of APs bring its corresponding design issues. For the orthogonal frequency-division multiple access (OFDMA) based RF AP, the binary allocation variables of the resource blocks (RB) make the resource allocation problem a mixed-integer nonlinear programming (MINP), which typically has prohibitive computational complexity [3]. With the unity frequency reuse across the VLC APs, the mutual interference among links results in a nonconvex signal-to-interference-plus-noise ratio (SINR), which makes the optimization problem NP-hard [4]. Second, due to the fact that each UE can get its service from VLC or RF, a deliberate network selection scheme should be jointly designed with the physical resource allocation scheme to explore both diverse UE requirements and AP characteristics. Furthermore, practical network optimization decisions must be made under stochastic channel conditions, traffic arrival rates and UEs' locations, hence an adaptive resource optimization scheme should be designed for coping with these dynamics. Finally, VLC networks are commonly employed in indoor scenarios where users are normally moving with low mobility. Therefore, the VLC link conditions are changing at a larger timescale when comparing with the RF channels. Moreover, the network selection in practical wireless networks are performed much more slowly than the resource allocation of RF AP, hence the two-timescale network decisions need to be operated by the operator, which is different from the widely studied single-timescale control [5]. These multiple factors make the resource optimization problem difficult to solve.

In this paper, we focus on the resource optimization of a HetNet combining with an RF and multiple VLCs. In this HetNet, both the RF wireless channel and the traffic arrival are changing at the small timescale, while the VLC channel

Manuscript received July 14, 2017; revised December 28, 2017 and March 11, 2018; accepted April 16, 2018. Date of publication April 30, 2018; date of current version November 16, 2018. This work was supported by NSF China (61471287, 61671062) and also supported by Eiffel scholarship under the auspices of CERI-LIA (Computer Science Laboratory), University of Avignon. The associate editor coordinating the review of this paper and approving it for publication was M. Abdallah. *(Corresponding author: Qinghai Yang.)*

W. Wu and Q. Yang are with the State Key Laboratory of ISN, Collaborative Innovation Center of Information Sensing and Understanding, School of Telecommunications Engineering, Xidian University, Xian 710071, China (e-mail: qhyang@xidian.edu.cn).

F. Zhou is with CERI-LIA, University of Avignon, 84000 Avignon, France, and also with the LISITE Laboratory, Institut Supérieur d'Electronique de Paris, Paris, France (e-mail: fen.zhou@univ-avignon.fr).

Color versions of one or more of the figures in this paper are available online at http://ieeexplore.ieee.org.

Digital Object Identifier 10.1109/TCOMM.2018.2831207

is changing at the large timescale. The minimization of the overall average power consumption is formulated as a two-timescale stochastic network resource optimization problem. With the help of multi-timescal Lyapunov optimization technique [6], the stochastic network resource optimization is decomposed into three corresponding subproblems. Specifically, at the large timescale, we obtain the network selection subproblem for the UEs and as well the joint transmission scheduling and power control subproblem for the VLC APs. At the small timescale, we obtain the joint RB and power allocation subproblem for the RF AP. Then, all of these subproblems are optimized to accommodate the stochastic network states.

The main contributions of this paper are summarized as follows:

- We propose an adaptive two-timescale resource optimization framework for the HetNet, where the large timescale network selection of the UEs, the transmission scheduling and power control of the VLC APs, and as well the small timescale RB and power allocation of the RF AP are jointly optimized to minimize the overall average transmit power consumption meanwhile stabilizing the network. It should be noted that the resource optimization framework does not require any prior-knowledge of the statistic of network states. Moreover, to the best our knowledge, it is the first time that the adaptive two-timescale resource optimization framework is proposed for the mixed RF/VLC HetNet.
- We develop a simple and convenient strategy for the network selection subproblem, which has the closed-form solution and is executed just by some comparison operations. Moreover, the optimal solution is given for the MINP problem of the RF AP, and a time-effective and easy-to-realize algorithm is proposed for the NP-hard joint transmission scheduling and power control problem of the VLC APs, both of which have an acceptable computational complexity.
- The proposed two-timescale resource optimization framework can adaptively handle the stochastic networks states and achieve a tradeoff between network power consumption and delay. Only by adjusting a control parameter, the proposed framework provides a controllable method to balance the power-delay performance and let the network operate in a predefined state.

The organization of the rest of this paper is as follows. In Section II, we present the related work. The network model and problem formulation are given in Section III. The resource optimization framework is proposed in Section IV. The network selection algorithm for UEs and the resource allocation algorithms for RF and VLC APs are given in Section V. Then, we present the simulation results to evaluate the proposed scheme. Finally, the conclusion is drawn in Section VII.

II. Related Work

The VLC system for wireless transmission has received growing research attentions in these years. It is reported that there are hundreds of teraHertz of free bandwidth completely untapped for communication in the VLC system [7], which provides an opportunity in designing high-capacity mobile data networks. By employing different transmission schemes, [8] investigated various VLC cell formations. An energy efficient indoor VLC system was designed in [9] by considering three interlinked design aspects, namely the cell formation, the link-level transmission and the system-level power allocation. Several modulation formats, such as on-off keying, pluse-position modulation and subcarrier modulation, were discussed in [10] for the VLC transmitters and receivers. The indoor visible light downlink scheme in [11] discussed the high quality video stream problems. However, all of these works pay their attentions only on the VLC system, which provide a finite range of coverage for the UEs. Hence the reliability of these systems is not optimistic.

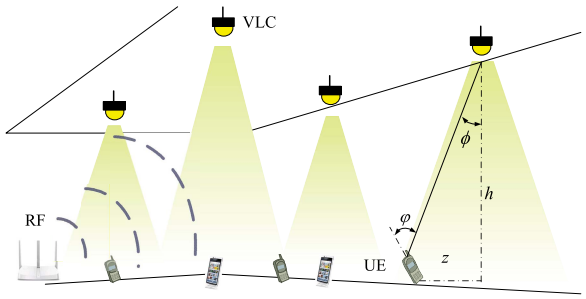

Fig. 1. System model.

The integrated network schemes in [12] and [13] demonstrated that the coexisting of VLC and RF allow the benefits of VLC to enhance traditional RF systems by increasing system bandwidth. Cooperative load balancing (LB) achieving proportional fairness (PF) was implemented in [14] for hybrid VLCs and WiFi. The hybrid VLC/RF systems were designed in [15] to achieve certain rate and reliability requirements. The resource-allocation problems of UEs are investigated in [16] and [17] for a HetNet deployed with both VLC and RF femtocell systems. However, these works neglect that both the RF wireless channels and the VLC channels are time-varying due to UE moving, channel fading and terminal shaking. Although some stochastic characteristics, such as moving UE and stochastic traffic arrivals, were considered in [18], [19], and [20], they only consider single timescale network operations. In practice, the network control decisions usually evolve in mixed timescales in wireless networks, such as power control adapts to the instantaneous channel state information (CSI) at the small timescale and the flow rate adapts to the CSI statistics at the large timescale [21]. By operating all of the network control decisions at the same timescale, these schemes [18]–[20] not only consumed a lot of computational resource but also incurred unacceptable iteration overheads. In contrast, our work considers that the network selection for UEs, the joint transmission scheduling and power control for VLC APs and as well the joint RB and power allocation for RF AP are determined in two timescales, which has never been studied in the literature.

III. System Model

We consider a HetNet, as shown in Fig. 1, which consists of one RF AP and N VLC APs. The UE is equipped

TABLE I
DEFINITIONS OF NOTATIONS

Symbol	Definition
$\mathcal{M}$, $\mathcal{N}$	Sets of UEs and APs
M, N	Numbers of UEs and APs
$\mathcal{N}_{RF}$, $\mathcal{N}_{vlc}$	Sets of RF AP and VLC APs
$\mathcal{T}_k$	The set of timeslots at frame k
$\alpha_{n,m}(kT)$	Network selection indicator between UE m and AP n during the k-th frame
$\mathcal{J}$	RB set of the RF AP
$x^i_{0,m}(t)$	Allocation indicator of RB i to UE m at timeslot t
$g^i_{0,m}(t)$	Channel gain between RF and UE m at timeslot t
$g_{n,m}(kT)$	Channel gain between VLC AP n and UE m at frame k
$p^i_{0,m}(t)$	Transmit power between RF and UE m at timeslot t
Υ	Channel capacity gap from Shannon bound
W, W_0	Bandwidths of RF system and RB
$\sigma^2_{RF}, \sigma^2_{vlc}$	Noise powers of RF AP and VLC AP
$u^i_{0,m}(t)$	Transmission rate between RF AP and UE m over RB i at timeslot t
$u_{n,m}(t)$	Transmission rate between AP n and UE m at timeslot t
$R_{0,m}(t)$	Transmission rate between RF and UE m at timeslot t
$R_{n,m}(t)$	Transmission rate between AP n and UE m at timeslot t
P_0^{max}	Instantaneous transmit power constraint of RF AP
P_n	Total optical power of VLC AP n
P_n^{dc}	DC power of VLC AP n
P_n^o	Signal optical power of VLC AP n
P_n^e	Electronic transmit power of VLC AP n
P_n^{min}, P_n^{max}	Dynamic range of a vishay TSHG8200 LED
$P_n^{o,max}$, $P_n^{e,max}$	Maximum optical power and maximum electronic power of VLC AP n
L_{min}	Minimum illumination requirement
$h^{illu}_{n,u}$	Luminous flux of unit optical power of VLC AP n provided by the uth point
P_n^e	Electronic transmit power of VLC AP n
$P^r_{n,m}$, $P^{r,e}_{n,m}$	Received optical power and electronic power from VLC AP n to UE m
$\xi_{n,m}$	SINR for UE m corresponding to VLC AP n
$C_{n,m}$	Channel capacity from VLC AP n to UE m
$A_m(t)$	The amount of data arrivals at timeslot t for UE m
$Q_{n,m}(t)$	Queue length maintained by AP n for UE m at timeslot t
$PC_n^{vlc}(t)$	Power consumption of VLC AP n at timeslot t
$PC^{RF}(t)$	Power consumption of RF AP at timeslot t

with both VLC receiver and RF receiver. The set of UEs is denoted by $\mathcal{M} = \{1, 2, \cdots, M\}$. Furthermore, we use $\mathcal{N} = \mathcal{N}_{RF} + \mathcal{N}_{vlc} = \{0, 1, 2, \cdots, N\}$ to denote the set of APs, where $\mathcal{N}_{RF} = \{0\}$ and $\mathcal{N}_{vlc} = \{1, 2, \cdots, N\}$ represent the set of RF AP and VLC APs, respectively. The RF channels are stochastic in both time and space due to shadowing and multipath effects, the coherence time is approximately 8.46-25.39ms [22]. The VLC channels are changing according to the users locations, angles of irradiation and incidence, the coherence time is approximately 0.05-0.2s [23]. Due to the fact that frequent switch among different APs will incur a nonnegligible cost, we assume that both the network selection and resource allocation of VLC APs are operated at the large timescale and that the resource allocation of the RF AP is operated at the small timescale. As shown in Fig. 2, we refer every T time slots as one frame and the k-th frame contains a set $\mathcal{T}_k = \{kT, kT+1, \cdots, kT+T-1\}$ of timeslots. It is assumed that both the network selection and resource allocation of VLC APs are determined at the beginning of each frame. Let the binary $\alpha_{n,m}(kT)$ be the network selection variable, where $\alpha_{n,m}(kT) = 1$ means that UE m is connected with AP n during the k-th frame and $\alpha_{n,m}(kT) = 0$ otherwise. Based on the fact that the UEs do not have the multi-homing capacity, we have the following constraint for $\alpha_{n,m}(kT)$:

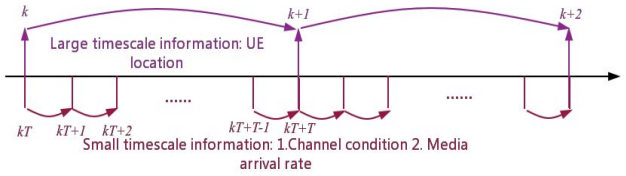

Fig. 2. Two timescale of network states, where the UEs locations are changing at the large timescale, while the RF channel conditions and the traffic arrival rates are changing at the small timescale.

$$\text{C1}: \sum_{n\in\mathcal{N}} \alpha_{n,m}(kT) = 1, \quad \alpha_{n,m}(kT) \in \{0,1\}, \ \forall m, \quad (1)$$

which means that UE m can only connect with one AP at each frame. TABLE I lists notation in this paper.

A. RF Model

Borrowing from the OFDM terminology, the radio resources of RF include resource blocks (RBs) and power. Let W and W_0 denote the system bandwidth and the bandwidth of each RB, respectively. Let $\mathcal{J}$ be the RB set of the RF AP and the number of RBs is J. Let $x^i_{0,m}(t)$ be the indicator function, where $x^i_{0,m}(t) = 1$ denotes that RB i of the RF AP is allocated for UE m, and $x^i_{0,m}(t) = 0$ otherwise. For RB i in the RF AP at timeslot t, we use $g^i_{0,m}(t)$ and $p^i_{0,m}(t)$ to denote the channel gain and transmit power for UE m, respectively. Then, the transmission rate between the RF AP and UE m over RB i at timeslot t is

$$u^i_{0,m}(t) = W_0 \log_2\left(1 + \Upsilon \frac{p^i_{0,m}(t) g^i_{0,m}(t)}{\sigma^2_{RF}}\right), \quad (2)$$

where Υ is the capacity gap from the Shannon channel capacity, and σ^2_{RF} is the noise power [3]. Therefore, the transmission rate between the RF AP and UE m is

$$\begin{aligned} R_{0,m}(t) &= \alpha_{0,m}(kT) u_{0,m}(t) \\ &= \alpha_{0,m}(kT) \sum_{i\in\mathcal{J}} x^i_{0,m}(t) u^i_{0,m}(t). \end{aligned} \quad (3)$$

Due to the fact that each RB can be allocated to at most one UE at each timeslot, then for any RB $i \in \mathcal{J}$, we have

$$\text{C2}: \sum_{m\in\mathcal{M}} \alpha_{0,m}(kT) x^i_{0,m}(t) \le 1, \quad x^i_{0,m}(t) \in \{0,1\}. \quad (4)$$

Let P_0^{max} be the instantaneous transmit power constraint of the RF AP, then we have the following constraint

$$\begin{aligned} \text{C3}: PC^{RF}(t) &= \sum_{m\in\mathcal{M}} \alpha_{0,m}(kT)p_{0,m}(t) \\ &= \sum_{m\in\mathcal{M}} \alpha_{0,m}(kT)\sum_{i\in\mathcal{J}} x_{0,m}^{i}(t)p_{0,m}^{i}(t) \le P_0^{max}. \end{aligned} \tag{5}$$

B. VLC Model

Let $g_{n,m}(kT)$ denote the VLC channel gain in indoor scenarios. It is shown in Fig. 1 that the VLC channel gain is determined by some light parameters, for example the angles of irradiation and incidence, the physical area of the photodiode (PD) on the UE, the distance between VLC AP and UE [18]. The communication signal of VLC is transmitted in the form of optical power, which should be positive and real. Therefore, the total optical power of VLC AP n can be denoted as $P_n = P_n^{dc} + P_n^o$, where P_n^{dc} is the direct current (DC) power for converting the bipolar signals into unipolar and P_n^o is the signal optical power. Moreover, we can find the DC bias power of each VLC by setting it at least as high as the minimum required optical power $P_{n,min}^{illu}$ for satisfying a predefined illumination requirement constituted by the minimum illumination L_{min}.

$$\begin{aligned} &\min \sum_{n\in\mathcal{N}_{vlc}} P_n \\ &\text{s.t.} \min_{u\in[1,K_p]} \sum_{n\in\mathcal{N}_{vlc}} P_n h_{n,u}^{illu} \ge L_{min}, \\ &\quad P_n^{min} < P_n < P_n^{max}, \end{aligned} \tag{6}$$

where $h_{n,u}^{illu}$ denotes the luminous flux of the unit optical power provided by the uth point of the K_p equally partitioned receiver plane.

Then, by adjusting the DC bias component to just satisfy the predefined illumination requirement $P_n^{dc} = P_{n,min}^{illu}$, the maximum optical power is obtained as $P_n^{o,max} = P_n^{max} - P_{n,illu}^{min}, \forall n \in \mathcal{N}_{vlc}$. According to [24], when an ACO-OFDM scheme is employed, the relationship between the electronic transmit power P_n^e and optical transmit power P_n^o is defined as $P_n^e = \pi\,(P_n^o)^2$, where π is the responsivity of the photodioide. Hence, we can find the maximum electronic transmit power for each VLC AP as $P_n^{e,max} = \pi\,(P_n^{o,max})^2$.

C. Transmission Rate of VLC

The receiver at the UE is comprised of a PD and a transmission impedance amplifier. After removal of the DC component and followed by direct detection, the electronic current generated by the PD of the signal from AP n to UE m is given by $< i_{n,m}^{pd}(kT) >= \varepsilon P_{n,m}^r(kT)$, where $P_{n,m}^r(kT) = P_n^o(t)g_{n,m}(kT)$, ε is the optical to electrical (O/E) conversion factor and $P_{n,m}^r(kT)$ is the received optical power from VLC AP n to UE m.

Hence, we define the received electrical signal to interference plus noise power ratio (SINR) for the m-th UE corresponding to VLC AP n as

$$\begin{aligned} \xi_{n,m}(kT) &= \frac{P_{n,m}^{r,e}(kT)}{\sigma_{vlc}^2 + \sum\limits_{n'\in\mathcal{N}_{vlc},n'\neq n} P_{n',m}^{r,e}(kT)} \\ &= \frac{\pi(\varepsilon P_{n,m}^r(kT))^2}{\sigma_{vlc}^2 + \sum\limits_{n'\in\mathcal{N}_{vlc},n'\neq n} \pi(\varepsilon P_{n',m}^r(kT))^2} \\ &= \frac{\pi(\varepsilon P_n^o(kT)g_{n,m}(kT))^2}{\sigma_{vlc}^2 + \sum\limits_{n'\in\mathcal{N}_{vlc},n'\neq n} \pi(\varepsilon P_{n'}^o(kT)g_{n',m}(kT))^2} \\ &= \frac{\varepsilon^2 P_n^e(kT)g_{n,m}(kT)^2}{\sigma_{vlc}^2 + \varepsilon^2 \sum\limits_{n'\in\mathcal{N}_{vlc},n'\neq n} P_{n'}^e(t)g_{n',m}(kT)^2}, \end{aligned} \tag{7}$$

where $P_{n,m}^{r,e}(kT)$ is the received signal power and σ_{vlc}^2 is the noise of VLC system.

As detailed in [14], the channel capacity from VLC AP n to UE m is computed as

$$\begin{aligned} &C_{n,m}(kT) \\ &= B\log_2\left(1+\frac{\varepsilon^2 P_n^e(kT)g_{n,m}(kT)^2}{\sigma_{vlc}^2+\varepsilon^2 \sum\limits_{n'\in\mathcal{N}_{vlc},n'\neq n} P_{n'}^e(kT)g_{n',m}(kT)^2}\right). \end{aligned} \tag{8}$$

In this work, the intra-cell orthogonal access is considered. This means that each VLC AP serves its neighboring UEs using orthogonal FDMA/TDMA. We define the channel coding rates between VLC AP n and UE m as $u_{n,m}(kT)$. Hence, the transmission rate from VLC AP n to UE m at timeslot t is computed as

$$R_{n,m}(t) = \alpha_{n,m}(kT)u_{n,m}(kT). \tag{9}$$

Based on orthogonal FDMA/TDMA, the set of rates $\{u_{n,m}(kT) : m \in \mathcal{M}\}$ is constrained to be in the "time-sharing region" of the broadcast channel formed by VLC AP n and its neighbors $\mathcal{M}$ [25]. It follows that the feasible channel coding rates $u_{n,m}(kT), \forall m \in \mathcal{M}$ for each VLC AP n must satisfy the constraint

$$\text{C4}: \sum_{m\in\mathcal{M}} \frac{\alpha_{n,m}(kT)u_{n,m}(kT)}{C_{n,m}(kT)} = 1, \quad \forall n \in \mathcal{N}_{vlc}, \tag{10}$$

and the transmit power constraint between VLC AP n and UE m can be represented as

$$\text{C5}: p_{n,m}(kT) = \frac{u_{n,m}(kT)}{C_{n,m}(kT)} P_n^e(kT) \le P_n^{e,max}. \tag{11}$$

Then, the power consumption of VLC AP n at timeslot t is modeled as

$$PC_n^{vlc}(t) = \sum_{m\in\mathcal{M}} \alpha_{n,m}(kT)p_{n,m}(kT) = P_n^e(kT), \tag{12}$$

where $\alpha_{m,n}(kT)$ is the network selection variable in Eq. (1).

D. Traffic Model and Queue Stability

We assume that separate buffering queues are maintained by the APs for each UE. Let $Q_{n,m}(t)$ denote the queue length maintained by AP n for UE m. The amount of data traffic arrivals at timeslot t for UE m is represented as $A_m(t)$. We assume that $\mathbf{A}(t) = [A_m(t)]_{m\in\mathcal{M}}$ is independently and identically distributed (i.i.d.) over different time-slots and that $\mathbf{A}(t)$ has the average arrival rate $\boldsymbol{\lambda} = [\lambda_m]_{m\in\mathcal{M}}$, i.e., $\mathbb{E}[A_m(t)] = \lambda_m, \forall m \in \mathcal{M}$. Hence, the queue process evolves according to (unit: bit)

$$Q_{n,m}(t+1) = \max[Q_{n,m}(t) - R_{n,m}(t), 0] + \alpha_{n,m}(kT)A_m(t). \quad (13)$$

Then, the general definition of queuing stability is given as follows.

Definition 1: A queue is defined as strongly stable [26] if

$$\lim_{T\to\infty}\frac{1}{T}\sum_{t=0}^{T-1}\mathbb{E}[Q_{n,m}(t)] < \infty. \quad (14)$$

Then, we can give the definition of network stable as that if all individual queues of the network are strongly stable.

E. Problem Formulation

In mixed RF/VLC system, supporting wireless communications should not violate the main illumination requirements of the VLC. Hence, the communications-related power should be as low as possible in order to minimize the perturbations imposed on the lightening function [9]. However, if we greedily minimize communications-related power, the bursty arrival of the data source as well as the associated delay performance will be ignored, which is very important for real-time applications. Based on the Little's Law [27], the average delay of the mobile user is given by the average backlog of the queue. As a result, there is no loss of generality to study the queue length for the purpose of minimizing the transmission delay. Therefore, in this paper, we focus on adaptively controlling the network resource allocation decisions for reducing communications-related power consumption while minimizing the queue lengths (or delay), i.e. making the network stable. Intuitively, the total transmit power consumption of the HetNet at timeslot t is computed as

$$P_{total}(t) = PC^{RF}(t) + \sum_{n\in\mathcal{N}_{vlc}} PC_n^{vlc}(t). \quad (15)$$

Then, we get the following stochastic optimization problem.

$$\begin{aligned}&\min\ \overline{P}_{total} = \lim_{T\to\infty}\frac{1}{T}\sum_{t=0}^{T-1}\mathbb{E}[P_{total}(t)]\\ &\text{s.t. } \overline{Q}_{n,m} = \lim_{T\to\infty}\frac{1}{T}\sum_{t=0}^{T-1}\mathbb{E}[Q_{n,m}(t)] < \infty, \quad \forall n, m,\\ &\quad \text{constraints C1} - \text{C5}. \end{aligned} \quad (16)$$

In realistic HetNet, the bursty traffic arrivals are time-varying and unpredictable, and both the long-term RF channel gain and the long-term VLC channel gain are very hard to capture. These characteristics make the problem infeasible to solve in an offline and integrated manner. Even more, the computational complexity of integrated solution will increase with the deployment of the number of the VLC APs. Therefore, it is imperative to design an online[1] and decomposition solution to make decisions effectively on joint RBs and power allocation for the RF AP, joint transmission scheduling and power control for the VLC APs and network selection for UEs.

IV. Algorithm Design Using Lyapunov Optimization

There are various approaches to deal with the stochastic resource optimization in wireless networks. One approach is the Markov Decision Process (MDP). In some special cases, it may be possible to obtain simple adaptive resource allocation solutions [28], [29]. However, the main issue associated with the MDP approach is that it cannot guarantee the network stability, whilst reveal the relationship between network stability and optimization objective. Compared with the MDP approach, Lyapunov optimization theory can enable stability and performance optimization to be treated simultaneously [30].

Before the algorithm design, we give the following introduction about Lyapunov optimization. Lyapunov optimization considering the stochastic network environment, makes online decisions while minimizing queue length and solving network utility optimization problem. Firstly, the drift function is defined to represent the difference between any adjacent slot queue, then the optimization objective is mapped into a penalty function. By minimizing the drift and penalty term, Lyapunov optimization can minimize the queue length and solve the network utility optimization problem. Lyapunov optimization is widely used for solving scheduling and resource allocation problems in stochastic networks, mainly due to its low computational complexity even for a stochastic system with a large number of system states. Moreover, Lyapunov optimization does not require the prior knowledge on the statistical information of the system randomness.

We firstly should demonstrate how the centralized stochastic optimization problem (16) can be decomposed into three separated problems, so that the corresponding problems can be solved independently of other parts.

Let $\mathbf{Q}(t) = [Q_{n,m}(t)]_{(N+1)\times M}$. We define the quadratic Lyapunov function as

$$L(\mathbf{Q}(t)) = \frac{1}{2}\sum_{n\in\mathcal{N}}\sum_{m\in\mathcal{M}} Q_{n,m}^2(t), \quad (17)$$

where $L(\mathbf{Q}(t))$ is the sum of the squares of all $Q_{n,m}(t)$. Hence, $L(\mathbf{Q}(t))$ is a scalar.

Different from the traditional Lyapunov optimization method in [26], which defines the Lyapunov drift at timeslot t, we define the T-timeslot (k-frame) conditional expected

[1] In this paper, "online" means that the algorithm relies on limited or no future channel state information (CSI) and queue state information (QSI). On the contrary, "offline" algorithm must require complete future CSI and QSI. Practically, it is not possible for the operator to know all future information on the system randomness, so we focus on the study of the online algorithm in this paper.

Lyapunov drift as

$$\Delta_T(\mathbf{Q}(t)) :\triangleq \mathbb{E}[L(\mathbf{Q}(t+T))|\mathbf{Q}(t)] - \mathbb{E}[L(\mathbf{Q}(t))]. \quad (18)$$

It can be easily found that the Lyapunov drift is a scalar. The Lyapunov drift shows the expected evolving direction[2] of the Lyapunov function $L(\mathbf{Q}(t))$ from the current state $\mathbf{Q}(t)$. For example, when the drift is negative, $\mathbf{Q}(t)$ is most likely decreasing and so that the queues are stable. We add the penalty term $V\mathbb{E}[\sum_{\tau=kT}^{kT+T-1} P_{total}(\tau)|\mathbf{Q}(kT)]$ to Eq. (18) for obtaining the following *drift-plus-penalty* term

$$\Delta_V(\mathbf{Q}(kT)) = \Delta(\mathbf{Q}(kT)) + V\mathbb{E}[\sum_{\tau=kT}^{kT+T-1} P_{total}(\tau)|\mathbf{Q}(kT)], \quad (19)$$

where $Q(kT)$ is the queue length $\mathbf{Q}(t)$ at the beginning of frame k, $V > 0$ is a control parameter. A larger V means that the optimization emphasizes more on power minimization compared to queue stability. On the contrary, it emphasizes more on queue stability than power minimization. By adjusting V, flexible design choices among various tradeoff points can be achieved by operators. In the drift-plus-penalty, minimizing the drift function at any time will limit the continuous growth of the queue to make the queue bounded and thus guarantee that the system satisfies the stable condition. The penalty function is a map of optimization objective. Therefore, Lyapunov's idea is to control the system strategy at any time to minimize the drift-plus-penalty term for making the queue stable, whilst minimizing the network power cost.

Then, we have the following lemma regarding the *drift-plus-penalty* term.

Lemma 1: For any feasible network resource allocation decisions $\mathbf{x}(\tau) = [x^i_{0,m}(\tau)]_{M\times J}$, $\mathbf{p}(\tau) = [p_{0,m}(\tau)]_{M\times J}$, $\mathbf{u}(kT) = [u_{n,m}(kT)]_{N_{vlc}\times M}$, $\mathbf{P}^e(kT) = [P^e_n(kT)]_{N_{vlc}\times 1}$, *and* $\boldsymbol{\alpha}(kT) = [\alpha_{n,m}(kT)]_{(N+1)\times M}$ *that can be implemented at timeslot* $\tau \in \mathcal{T}_k$, *we can obtain the following equation*

$$\begin{aligned}
&\Delta_V(\mathbf{Q}(kT)) \\
&\le B_1T + \mathbb{E}\Bigg\{V\sum_{\tau=kT}^{\tau=kT+T-1} P_{total}(\tau) + \sum_{n,m}\sum_{\tau=kT}^{\tau=kT+T-1} Q_{n,m}(\tau) \\
&\quad \times(\alpha_{n,m}(kT)A_m(\tau) - R_{n,m}(\tau))|\mathbf{Q}(kT)\Bigg\} \quad (20)\\
&\le B_2T + \mathbb{E}\Bigg\{V\sum_{\tau=kT}^{\tau=kT+T-1} P_{total}(\tau) + \sum_{n,m}\sum_{\tau=kT}^{\tau=kT+T-1} Q_{n,m}(kT) \\
&\quad \times\ (\alpha_{n,m}(kT)A_m(\tau) - R_{n,m}(\tau))|\mathbf{Q}(kT)\Bigg\}, \quad (21)
\end{aligned}$$

[2]The "evolving direction" shows the trends of increase or decrease about the Lyapunov function $L(\mathbf{Q}(t))$. Negative drift indicates $\mathbb{E}[L(\mathbf{Q}(t+T))|\mathbf{Q}(t)] - \mathbb{E}[L(\mathbf{Q}(t))] < 0$, which shows a decrease "evolving direction", so $\mathbf{Q}(t)$ is most likely decreasing. While positive drift means $\mathbb{E}[L(\mathbf{Q}(t+T))|\mathbf{Q}(t)] - \mathbb{E}[L(\mathbf{Q}(t))] > 0$, which indicates a increase "evolving direction", so the queue length $\mathbf{Q}(t)$ is most likely increasing.

where $\sum_{n,m}$ *is the simplification of* $\sum_{n=0}^{N}\sum_{m=1}^{M}$, $B_1 = \frac{(N+1)\times M}{2}(R^2_{max} + A^2_{max})$ *and* $B_2 = \frac{(N+1)\times M}{2}(R^2_{max} + A^2_{max})T$.

Proof: The similar proof can be found in [6]. ■

It can be found that the tightness of the bound in Lemma 1 is related to the constants B_1 and B_2, which illustrates that the tightness of the bound is determined by the node number in the network, the frame length and the traffic size. This is just consistent as the practical wireless networks, where the resource optimization in a large scale and heavy traffic wireless network is always relatively sketchier than the optimization in a small scale network with light traffic.

Then, by minimizing the upper bound of Eq. (21), we can solve the original optimization problem in (16), with V acting as a control parameter to determine the tradeoff between optimization objective and queue length. Based on observing some important features of Eq. (21), the following optimization scheme can be obtained. First, under given $\mathbf{Q}(kT)$, we should determine the network selection $\boldsymbol{\alpha}\ (kT)$ at the large timescale based on the optimal resource allocations $\mathbf{u}^*(kT)$, $\mathbf{P}^{e,*}(kT)$ and $\mathbf{x}^*(\tau)$, $\mathbf{p}^*(\tau)$ during timeslots $\tau \in [kT, kT+1, \cdots, kT+T-1]$. Upon determining the network selection $\boldsymbol{\alpha}^*(kT)$, the resource allocations can be further decomposed into two problems. When $n \in \mathcal{N}_{RF}$, we obtain the joint RB and power allocation problem for the RF AP at the small timescale. On the other hand, when $n \in \mathcal{N}_{vlc}$, we obtain the joint transmission scheduling and power control problem for VLC APs at the large timescale.

Based on the analysis above, we propose a two stage backward induction framework for the RF/VLC network resource optimization. At the beginning of each frame, the two stage backward induction framework first make the network selection decisions (stage 1), and then ponders all subsequent reactions of the resource allocations about RF and VLC APs (stage 2). Based on the optimal resource allocations at stage 2, the framework can solve the network selection variables again (stage 1), then based on the network selection variables, the framework will find the corresponding resource allocations (stage 2). In this way, stage 1 and stage2 are iteratively executed until the optimal network optimization variables are found. Here we assume that the operator can predict the system randomness for the current frame. In fact, the recent information prediction models can accurately predict the system randomness for a time window that is more larger than the frame length [31], [32]. The similar perfect prediction assumption has been made in [33].

Then, we present the adaptive network resource optimization (ANRO) framework and illustrate its flowchart in Fig. 3.

A. Adaptive Network Resource Optimization Framework

1) Stage I (Network Selection): Observe the current queue length $\mathbf{Q}(kT)$ and the channel gains $\mathbf{G}^{RF}(t) = [g^i_{0,m}(t)]_{m\in\mathcal{M}, i\in\mathcal{J}}$, $\mathbf{G}^{vlc}(kT) = [g_{n,m}(kT)]_{n\in\mathcal{N}_{vlc}, m\in\mathcal{M}}$ in this frame and make the network selection decision

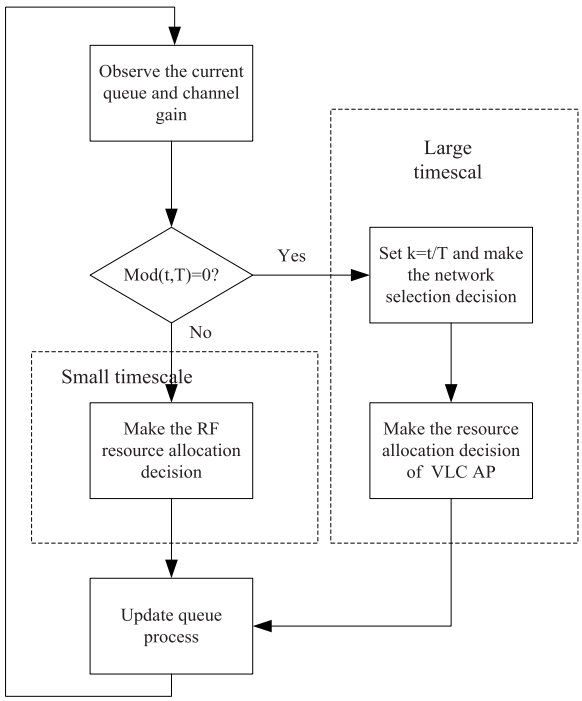

Fig. 3. Flowchart of ANRO.

according to

$$\min\left\{\begin{array}{c}\sum\limits_{n,m}\alpha_{n,m}(kT)Q_{n,m}(kT)\sum\limits_{\tau=kT}^{\tau=kT+T-1}(A_m(\tau)-u_{n,m}(\tau))\\ +\sum\limits_{n,m}\alpha_{n,m}(kT)\sum\limits_{\tau=kT}^{\tau=kT+T-1}Vp_{n,m}(\tau)\end{array}\right\}$$

$$\text{s.t.}\ \sum_{n\in\mathcal{N}}\alpha_{n,m}(kT)=1,\alpha_{n,m}(kT)\in\{0,1\},\quad\forall m\in\mathcal{M}. \tag{22}$$

2) Stage II (Resource Allocations About RF and VLC APs): Based on the given network selection $\boldsymbol{\alpha}(kT)$ and the channel gain $\mathbf{G}^{vlc}(kT)=[g_{n,m}(kT)]_{n\in\mathcal{N}_{vlc},m\in\mathcal{M}}$ in this frame, make the joint transmission scheduling and power control for VLC AP according to

$$\max\sum_{n\in\mathcal{N}_{vlc}}\sum_{m\in\mathcal{M}_n^k}\sum_{\tau=kT}^{kT+T-1}(Q_{n,m}(kT)u_{n,m}(kT)-Vp_{n,m}(kT))$$

$$\text{s.t.}\ \sum_{m\in\mathcal{M}}\frac{\alpha_{n,m}(kT)u_{n,m}(kT)}{C_{n,m}(kT)}=1,\quad\forall n\in\mathcal{N}_{vlc},$$

$$p_{n,m}(kT)\le P_n^{e,max},\quad\forall n\in\mathcal{N}_{vlc},\ m\in\mathcal{M}_n^k, \tag{23}$$

where $\mathcal{M}_n^k$ is the set of UEs connected with VLC AP n at frame k.

Based on the given network selection $\boldsymbol{\alpha}(kT)$ and the channel gain $\mathbf{G}^{RF}(t)=[g_{0,m}^i(t)]_{m\in\mathcal{M},i\in\mathcal{J}}$ in this frame, make the joint RB and power allocation for RF AP according to

$$\max\sum_{m\in\mathcal{M}_0^k}Q_{0,m}(kT)\sum_{\tau=kT}^{kT+T-1}u_{0,m}(\tau)-\sum_{m\in\mathcal{M}_0^k}\sum_{\tau=kT}^{kT+T-1}Vp_{0,m}(\tau)$$

$$\text{s.t.}\ \sum_{m\in\mathcal{M}_0^k}x_{0,m}^i(\tau)\le 1,x_{0,m}^i(\tau)\in\{0,1\},$$

$$\sum_{m\in\mathcal{M}_0^k}\sum_{i\in\mathcal{J}}x_{0,m}^i(\tau)p_{0,m}^i(\tau)\le P_0^{max}, \tag{24}$$

where $\mathcal{M}_0^k$ is the set of UEs connected with the RF AP at frame k.

Under the adaptive network resource allocation framework, the original problem achieves complete separation, of which the separated problems can be solved by distributed approach. In the following section, we will discuss the handling of each of these problems.

V. Design of Adaptive Network Resource Allocation

In this section, we develop an effective method to solve the network selection, joint transmission scheduling and power control and as well the joint RB and power allocation problems separately.

A. Network Selection

It is shown in problem (22) that the network selection is independent among different UEs. Thus, problem (22) can be equivalently decomposed into M subproblems, each of which is given as

$$\min\sum_{n=0}^{N}\alpha_{n,m}(kT)z_{n,m}(kT)$$

$$\text{s.t.}\ \sum_{n=0}^{N}\alpha_{n,m}(kT)=1,\quad\alpha_{n,m}(kT)\in\{0,1\}, \tag{25}$$

where $z_{n,m}(kT)=$

$$Q_{n,m}(kT)\sum_{\tau=kT}^{\tau=kT+T-1}(A_m(\tau)-u_{n,m}(\tau))+\sum_{\tau=kT}^{\tau=kT+T-1}Vp_{n,m}(\tau).$$

This is a linear optimization problem, whose solution is given as follows

$$\alpha_{n,m}(kT)=\begin{cases}1, & n=\underset{l}{\operatorname{argmin}}\{z_{l,m}(kT),0\le l\le N\},\\ 0, & \text{otherwise.}\end{cases} \tag{26}$$

Under the network selection strategy above, $z_{n,m}(kT)$ can be considered as the congestion cost for AP n serving UE m during frame k. Then, Eq. (26) ensures that the UE connects to the AP with smallest congestion cost.

Algorithm 1 Joint Transmission Scheduling and Power Control Algorithm

Initialization

- Set $i=0$, initialize $\mathbf{v}(0)$ and $\mathbf{P}^e(0)$, set the maximum tolerances $\varpi>0$.

while $|\Psi\ (\mathbf{v}(i+1),\mathbf{P}^e(i+1))-\Psi\ (\mathbf{v}(i),\mathbf{P}^e(i))|\geq\varpi$ **do**

Step 1: Derive $\mathbf{v}(i)^*$ from Eq. (30);

Step 2: For derived $\mathbf{v}(i)^*$, find $\mathbf{P}^e(i)^*$ from (31) by applying **Algorithm 2**;

Step 3: Set $i=i+1$ and calculate $\Psi\ (\mathbf{v}(i+1),\mathbf{P}^e(i+1))$.

end while

B. Joint Transmission Scheduling and Power Control for VLC APs

It is shown in (23) that the joint transmission scheduling and power control problems have no relationship with the timeslots τ. Hence, it can be rewritten as

$$\begin{aligned}&\max \sum_{n\in\mathcal{N}_{vlc}}\sum_{m\in\mathcal{M}_n^k}(Q_{n,m}(kT)u_{n,m}(kT)-Vp_{n,m}(kT))\\&\text{s.t.}\sum_{m\in\mathcal{M}}\frac{\alpha_{n,m}(kT)u_{n,m}(kT)}{C_{n,m}(kT)}=1,\quad\forall n\in\mathcal{N}_{vlc},\\&\quad p_{n,m}(kT)\leq P_n^{e,max},\quad\forall n\in\mathcal{N}_{vlc},\ m\in\mathcal{M}_n^k.\end{aligned}\tag{27}$$

By introducing the transmission scheduling variable $\mathbf{v}=[v_{n,m}]_{n\in\mathcal{N}_{vlc},m\in\mathcal{M}}$ and $v_{n,m}(kT)=\frac{u_{n,m}(kT)}{C_{n,m}(kT)}$, it reduces to

$$\begin{aligned}&\max\Psi\ (\mathbf{v},\mathbf{P}^e)\\&\text{s.t.}\sum_{m\in\mathcal{M}}v_{n,m}=1,\quad\forall n\in\mathcal{N}_{vlc},\\&\quad v_{n,m}P_n^e\leq P_n^{e,max},\quad\forall n\in\mathcal{N}_{vlc},\ m\in\mathcal{M}_n^k,\end{aligned}\tag{28}$$

where $\Psi\ (\mathbf{v},\mathbf{P}^e)=\sum_{n\in\mathcal{N}_{vlc}}\sum_{m\in\mathcal{M}_n^k}v_{n,m}(Q_{n,m}C_{n,m}-VP_n^e)$, the time index kT is omitted for the sake of simplicity.

Optimization problem (28) has coupling constraint with transmission scheduling variable $\mathbf{v}$ and power control variable $\mathbf{P}^e$. To tackle the computational complexity of (28), we propose an iterative approach to find the optimal solution, which has been widely used for coupling resource optimization problems in wireless network [34], [35]. As shown in **Algorithm 1**, in the first step, the scheduling variable $v_{n,m}$ is obtained under a given power control vector $\mathbf{P}^e$. This derived scheduling variable $v_{n,m}$ is then used in the second step to find the corresponding power control $\mathbf{P}^e$ as the solution of the power control problem. Steps 1 and 2 are iteratively executed until the maximum of problem (28) is not much different from the previous iteration.

1) Transmission Scheduling: Denoting $H_{n,m}(\mathbf{P}^e)=Q_{n,m}C_{n,m}-VP_n^e$, the transmission scheduling problem for given $\mathbf{P}^e$ becomes

$$\begin{aligned}&\max\sum_{n\in\mathcal{N}_{vlc}}\sum_{m\in\mathcal{M}_n^k}v_{n,m}H_{n,m}(\mathbf{P}^e)\\&\text{s.t.}\sum_{m\in\mathcal{M}}v_{n,m}=1,\forall n\in\mathcal{N}_{vlc}.\end{aligned}\tag{29}$$

Problem (29) is a classical linear assignment problem, whose solution can be given as

$$v_{n,m_n}=\begin{cases}1, & m_n=\underset{l}{\operatorname{argmax}}\{H_{n,l}(\mathbf{P}^e),l\in\mathcal{M}_n^k\},\\0, & \text{otherwise.}\end{cases}\tag{30}$$

In Eq. (30), $H_{n,m}(\mathbf{P}^e)$ can be interpreted as the energy-efficiency for UE m associating to VLC AP n. Thus, we can find that the solution consists of associating to the VLC AP with the largest energy-efficiency at each frame, which agrees with our objective of power minimization. Moreover, this UE will be served at the rate $u_{n,m}=C_{n,m}$, while all other UEs of this VLC AP are not served at this frame, which reflects the principle of TDMA.

2) Power Control: After determining the transmission scheduling variables, we obtain the following power control problem

$$\begin{aligned}&\max\sum_{n\in\mathcal{N}_{vlc}}Q_{n,m_n}B\log_2\left(1+\frac{\varepsilon^2P_n^eg_{n,m_n}^2}{\sigma_{vlc}^2+\varepsilon^2\sum\limits_{n'\in\mathcal{N}_{vlc},n'\neq n}P_{n'}^eg_{n',m_n}^2}\right)\\&\qquad-V\sum_{n\in\mathcal{N}_{vlc}}P_n^e\\&\text{s.t. }0\leq P_n^e\leq P_n^{e,max},\quad\forall n\in\mathcal{N}_{vlc}.\end{aligned}\tag{31}$$

Optimization problem (31) has a non-convex objective function due to inter-cell interference among different VLC APs. Conventional methods usually deal with the non-convex problem by directly applying the successive convex approximation (SCA) and then solving the resultant convex approximation problems by interior-point methods. However, the initial parameters and stepsizes in these methods need to be designed meticulously, which is usually a time-consuming process. Hence, it is imperative to design a time-efficient and easy-to-implement power control algorithm. In this subsection, we will approximate the non-convex objective function in the exponential domain of power. Through this way, the resultant approximation problem facilitates us to devise a fast algorithm that provably achieves at least local optimality.

Letting $\beta_n=\ln P_n^e$, the objective function of (31) can be reformulated as

$$\begin{aligned}&\sum_{n\in\mathcal{N}_{vlc}}Q_{n,m_n}B\log_2\left(\frac{\sigma_{vlc}^2+\varepsilon^2\sum\limits_{n'\in\mathcal{N}_{vlc}}e^{\beta_{n'}}g_{n,m_n}^2}{\sigma_{vlc}^2+\varepsilon^2\sum\limits_{n'\in\mathcal{N}_{vlc},n'\neq n}e^{\beta_{n'}}g_{n',m_n}^2}\right)\\&\qquad-V\sum_{n\in\mathcal{N}_{vlc}}e^{\beta_n}.\end{aligned}\tag{32}$$

Denoting

$$\begin{aligned}f_n(\boldsymbol{\beta})&=Q_{n,m_n}B\log_2\left(\sigma_{vlc}^2+\varepsilon^2\sum_{n'\in\mathcal{N}_{vlc}}e^{\beta_{n'}}g_{n',m_n}^2\right),\\y_n(\boldsymbol{\beta})&=Q_{n,m_n}B\log_2\left(\sigma_{vlc}^2+\varepsilon^2\sum_{n'\in\mathcal{N}_{vlc},n'\neq n}e^{\beta_{n'}}g_{n',m_n}^2\right)\\&\quad+Ve^{\beta_n},\end{aligned}$$

problem (31) is formulated as

$$\begin{aligned} &\max\ f(\boldsymbol{\beta}) - y(\boldsymbol{\beta}) \\ &\text{s.t.}\ \ 0 \le e^{\beta_n} \le P_n^{e,max}, \quad \forall n \in \mathcal{N}_{vlc}. \end{aligned} \tag{33}$$

where $f(\boldsymbol{\beta}) = \sum_{n\in\mathcal{N}_{vlc}} f_n(\boldsymbol{\beta})$ and $y(\boldsymbol{\beta}) = \sum_{n\in\mathcal{N}_{vlc}} y_n(\boldsymbol{\beta})$.

In optimization problem (33), both $f(\boldsymbol{\beta})$ and $y(\boldsymbol{\beta})$ are convex functions. Therefore, if $f(\boldsymbol{\beta})$ can be approximated by some linear functions, problem (33) can be reformulated as a concave optimization problem. Motivated by this consideration, we give the first-order Taylor expansion of $f(\boldsymbol{\beta})$ at the point $\boldsymbol{\beta}^l$, i.e.

$$f(\boldsymbol{\beta}) \approx f(\boldsymbol{\beta}^l) + \nabla f(\boldsymbol{\beta}^l)^T(\boldsymbol{\beta} - \boldsymbol{\beta}^l), \tag{34}$$

where

$$\nabla f(\boldsymbol{\beta}^l) = \left(\frac{\partial f(\boldsymbol{\beta})}{\partial \beta_n^l}\right)_{N_{vlc}\times 1}$$

and

$$\frac{\partial f(\boldsymbol{\beta})}{\partial \beta_n^l} = \sum_{n'\in\mathcal{N}_{vlc}} \frac{Q_{n',m_{n'}} B\varepsilon^2 e^{\beta_n} g_{n,m_{n'}}^2}{\left(\sigma_{vlc}^2 + \varepsilon^2 \sum\limits_{n''\in\mathcal{N}_{vlc}} e^{\beta_{n''}} g_{n'',m_{n'}}^2\right)\ln 2}.$$

Replacing $f(\boldsymbol{\beta})$ in Eq. (33) by Eq. (34), it yields

$$\begin{aligned} &\max\ f(\boldsymbol{\beta}^l) + \nabla f(\boldsymbol{\beta}^l)^T(\boldsymbol{\beta} - \boldsymbol{\beta}^l) - y(\boldsymbol{\beta}) \\ &\text{s.t.}\ 0 \le e^{\beta_n} \le P_n^{e,max}, \quad \forall n \in \mathcal{N}_{vlc}. \end{aligned} \tag{35}$$

Because the objective function of (35) is concave function and the constraint is convex set, thus problem (35) is concave optimization. Then, finding the derivative of the objective function of (35) with respect to $\boldsymbol{\beta}$ and making it to zero, we obtain Eq. (36) at the bottom of this page.

Based on the equation above, we give the following exponential domain approximated power control (EAPC) algorithm.

Due to the fact that problem (35) is a concave optimization, so that the convergence of Step 1 in **Algorithm 2** is guaranteed. The convergence of the successive approximation in Step 2 can be implemented only in a small number of iterations [36]. Hence, a cost-effective and easy-to-realized algorithm is given for the power control for VLC APs.

Algorithm 2 Exponential Domain Approximated Power Control (EAPC)

Initialization

- Set $i = 0$, $l = 0$, and the maximum tolerances $\nu > 0$ and $\zeta > 0$.
- Set the initial β^0.
- Calculate $I^0 = f(\boldsymbol{\beta}^0) - y(\boldsymbol{\beta}^0)$.

while $|I^l - I^{l-1}| \ge \nu$ **do**

Step 1: Repeat power control through Eq. (40) until $||\mathbf{P}^e(i+1) - \mathbf{P}(i)|| \le \zeta$;

Step 2: Set $l = l+1$, $\beta_n^l = \log\ (P_n^e(i+1))$, and $i = 0$;

Step 3: Calculate $I^{l+1} = f(\boldsymbol{\beta}^l) - y(\boldsymbol{\beta}^l)$.

end while

Finally, we should investigate the computational complexity of the joint transmission scheduling and power control. It is shown that **Algorithm 2** is nested in the joint transmission scheduling and power control algorithm (**Algorithm 1**). Therefore, we should provide the computational complexity of **Algorithm 2** firstly. In **Algorithm 2**, there are two loops executed nested. If we want to achieve ν-optimality in the inner loop, the number of iterations is on the order of $O(\frac{1}{\nu^2})$ [35]. Similarly, the computational complexity of the outer loop is $O(\frac{1}{\zeta^2})$. Therefore, the computational complexity of **Algorithm 2** can be considered as $O(\frac{1}{\nu^2\zeta^2})$. Then, together with **Algorithm 1**, where the maximum tolerances is ϖ, the computational complexity of the joint transmission scheduling and power control in Section V is $O(\frac{1}{\nu^2\zeta^2\varpi^2})$.

C. Joint RBs and Power Allocation for RF AP

We observe from problem (24) that the joint RBs and power allocation problems at the different timeslots $\tau \in \{kT, kT+1, \cdots, kT+T-1\}$ in frame k are independent of each other, so that problem (24) can be equivalently decomposed into T subproblems. Since the objective of problem (24) is the function of transmit power $p_{0,m}(\tau)$ and the binary variables $x_{0,m}^i(t)$, the joint RBs and power allocation problem is a mixed-integer non-linear convex programming, which typically has prohibitive computational complexity. In this paper, we will exploit the Lagrange relaxation method to solve

$$P_n^e = \min\left\{ \frac{\frac{\partial f(\boldsymbol{\beta})}{\partial \beta_n^l}}{\sum\limits_{n'\in\mathcal{N}_{vlc}, n'\ne n} \frac{Q_{n',m_{n'}} B\varepsilon^2 g_{n,m_{n'}}^2}{\left(\sigma_{vlc}^2 + \varepsilon^2 \sum\limits_{n''\in\mathcal{N}_{vlc}, n''\ne n'} P_{n''}^e g_{n'',m_{n'}}^2\right)\ln 2} + V}, P_n^{e,max} \right\} \tag{36}$$

$$P_n^e(i+1) = \min\left\{ \frac{\frac{\partial f(\boldsymbol{\beta})}{\partial \beta_n^l}}{\sum\limits_{n'\in\mathcal{N}_{vlc}, n'\ne n} \frac{Q_{n',m_{n'}} B\varepsilon^2 g_{n,m_{n'}}^2}{\left(\sigma_{vlc}^2 + \varepsilon^2 \sum\limits_{n''\in\mathcal{N}_{vlc}, n''\ne n'} P_{n''}^e(i) g_{n'',m_{n'}}^2\right)\ln 2} + V}, P_n^{e,max} \right\} \tag{37}$$

this problem. Moreover, the special structure of problem (27) allows us to derive the optimal solution.

1) Continuity Relaxation: We first relax $x^i_{0,m}(\tau)$ to the continuous interval $[0,1]$. After that, we define a new variable $s^i_{0,m}(\tau) = x^i_{0,m}(\tau)p^i_{0,m}(\tau)$. Then, problem (24) can be reformulated as a concave optimization problem

$$\begin{aligned}\max \sum_{m\in\mathcal{M}_0^k}\sum_{i\in\mathcal{J}_n} Q_{0,m}x^i_{0,m}W_0\log_2\left(1+\Upsilon\frac{s^i_{0,m}g^i_{0,m}}{x^i_{0,m}\sigma^2_{RF}}\right)\\ -\sum_{m\in\mathcal{M}_0^k} V\sum_{i\in\mathcal{J}} s^i_{0,m}\\ \text{s.t.}\sum_{m\in\mathcal{M}_0^k}\sum_{i\in\mathcal{J}} s^i_{0,m}\le P_0^{max}, s^i_{0,m}\ge 0,\\ \sum_{m\in\mathcal{M}_0^k} x^i_{0,m}\le 1,\quad x^i_{0,m}\in[0,1],\end{aligned} \tag{38}$$

where the time indexes kT and τ are omitted for the sake of simplicity.

2) Lagrange Duality: By relaxing the power constraint based on dual variables χ, we introduce the Lagrange of problem (38) as

$$\begin{aligned}&L(\chi,\mathbf{s}_0,\mathbf{x}_0)\\ &=\sum_{m\in\mathcal{M}_0^k}\sum_{i\in\mathcal{J}} Q_{0,m}x^i_{0,m}W_0\log_2\left(1+\Upsilon\frac{s^i_{0,m}g^i_{0,m}}{x^i_{0,m}\sigma^2_{RF}}\right)\\ &\quad-\sum_{m\in\mathcal{M}_0^k}\sum_{i\in\mathcal{J}} Vs^i_{0,m}-\chi(\sum_{m\in\mathcal{M}_0^k}\sum_{i\in\mathcal{J}} s^i_{0,m}-P_0^{max}),\end{aligned} \tag{39}$$

where $\mathbf{s}_0=[s^i_{0,m}]_{M\times J}$ and $\mathbf{x}_0=[x^i_{0,m}]_{M\times J}$.

Hence, the Lagrange dual function is

$$\begin{aligned}d(\chi) &= \max L(\chi,\mathbf{s}_0,\mathbf{x}_0)\\ &\text{s.t.}\sum_{m\in\mathcal{M}_0^k} x^i_{0,m}\le 1,\quad x^i_{0,m}\in[0,1],\ s^i_{0,m}\ge 0,\end{aligned} \tag{40}$$

and the dual problem of (38) is

$$\min\ d(\chi)\quad \text{s.t. } \chi\ge 0. \tag{41}$$

Based on the Karush-Kuhn-Tucker (KKT) conditions, the relationship between $\mathbf{s}_0$ and $\mathbf{x}_0$ can be written as

$$s^i_{0,m}=\left[\frac{Q_{0,m}W_0}{(V+\chi)\ln 2}-\frac{\sigma^2_{RF}}{\Upsilon g^i_{0,m}}\right]^+ x^i_{0,m}. \tag{42}$$

After substituting Eq. (42) into Eq. (40), we obtain

$$\begin{aligned}d(\chi)=\max &\sum_{m\in\mathcal{M}_0^k}\sum_{i\in\mathcal{J}_n}\Lambda^i_{0,m}x^i_{0,m}+\chi P_0^{max}\\ &\text{s.t.}\sum_{m\in\mathcal{M}_0^k} x^i_{0,m}\le 1, x^i_{0,m}\in[0,1],\end{aligned} \tag{43}$$

where $\Lambda^i_{0,m}(\chi) =$

$$\begin{aligned}&Q_{0,m}W_0\log_2\left(1+\Upsilon\frac{g^i_{0,m}}{\sigma^2_{RF}}\left[\frac{Q_{0,m}W_0}{(V+\chi)\ln 2}-\frac{\sigma^2_{RF}}{\Upsilon g^i_{0,m}}\right]^+\right)\\ &-V\left[\frac{Q_{0,m}W_0}{(V+\chi)\ln 2}-\frac{\sigma^2_{RF}}{\Upsilon g^i_{0,m}}\right]^+-\chi\left[\frac{Q_{0,m}W_0}{(V+\chi)\ln 2}-\frac{\sigma^2_{RF}}{\Upsilon g^i_{0,m}}\right]^+.\end{aligned} \tag{44}$$

It can be easily seen that problem (43) is a classical linear assignment problem, whose solution can be given as

$$x^i_{0,m}=\begin{cases}1, & m=\underset{l}{\text{argmax}}\{\Lambda^i_{0,l}(\chi), l\in\mathcal{M}_0\},\\ 0, & \text{otherwise.}\end{cases} \tag{45}$$

After computing the optimal RBs allocation $\mathbf{x}_0$, the optimal power allocation $\mathbf{p}_0$ can be obtained from Eq. (42). The optimal value of χ can be determined by solving dual problem (41). By using a subgradient method, the optimal value of χ is given by

$$\chi(\iota+1)=\chi(\iota)+\vartheta\left(\sum_{m\in\mathcal{M}_0^k}\sum_{i\in\mathcal{J}} p^i_{0,m}(\iota)-P_0^{max}\right), \tag{46}$$

where ι is the iteration index and ϑ is a sufficiently small positive step-size. Since the gradient of (41) satisfies the Lipchitz continuity condition, the convergence of (46) towards the optimal λ is guaranteed. Hence, the power allocation $\mathbf{p}_0$ can converge to the optimal solution.

Then, we should investigate the computational complexity for joint RB and power allocation. For solving the RF resource optimization problem, the subgradient method is utilized to solve dual problem (41). In order to achieve δ-optimality, i.e., $|d(\chi)-d(\chi^*)|<\delta$, the number of iterations is on the order of $O(1/\delta^2)$ [37]. In each iteration, Eq. (45) needs to be computed for J RBs. Because that there are M UEs connected to the AP, Eq. (45) needs to be computed $M\cdot J$ times in each iteration. Thus the computational complexity for joint RB and power allocation is $O\left(\frac{JM}{\delta^2}\right)$.

The convergence of the RFs resource allocation can be implemented in polynomial time. Moreover, we have mentioned that the proposed network selection strategy has a simple and convenient structure, which is executed just by some comparison operations. Besides, the joint transmission scheduling and power control algorithm is cost-effective and easy-to-realized. Therefore, our proposed resource optimization strategies under ANRO can find the optimal solutions quickly during each timeslot and can adapt to the traffic level dynamics, wireless channel fading and the random UE locations.

VI. Simulation Results

In this section, we present the simulations to evaluate the performance of our proposed adaptive network resource allocation scheme.

A. Parameters Setting

The values of RF and VLC are obtained from [11] and [38], respectively. We consider a simplified model of a 2-Dimensional (2D) room having the length of 16 [m] and the height of 3 [m]. There are 3 VLC APs installed on the ceiling at 9, 12 and 15 [m] for serving the UEs. The RF AP is deployed at 0 [m] of the room and it has 20 RBs. The path loss model of the RF AP is given by $31.5+35.0\log 10(d)$, where d denotes the distance between transmitter and receiver in meters. There are 10 UEs in the

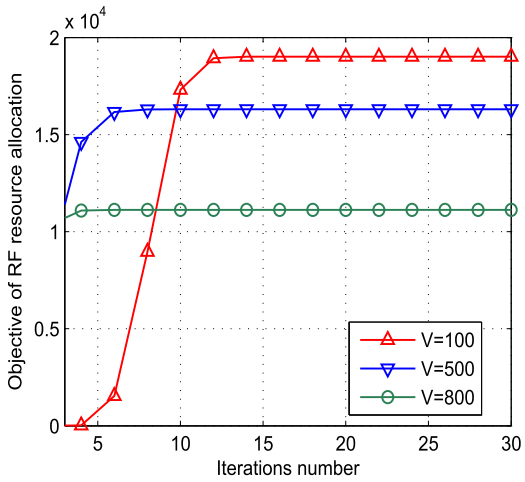

Fig. 4. Convergence speed of RF resource allocation algorithm under different Lyapunov term coefficient V.

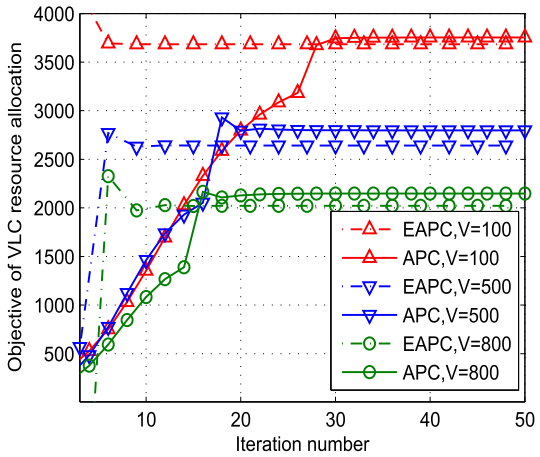

Fig. 5. Convergence speed of EAPC and APC algorithms under different Lyapunov term coefficient V.

simulation system, and they are randomly and uniformly distributed located such the distance to the RF AP is in the range between 1 and 16 meters. We assume that the fast channel fading coefficients are generated as i.i.d Gaussian random variables with unit variances. The noise power density is -76dBm/Hz. The maximum transmit power of the RF AP is given as $P_0^{max} = 10$W. In this simulation, one VLC has 40 LEDs, each of which has 300mW, hence the maximum power of the VLC AP is 12W. For simplicity of simulations, we consider a normalized RB spectral bandwidth, i.e. $W_0 = 1$Hz, so the system bandwidth of RF is $W = 20$Hz. For investigating the illumination requirements, we partition 3 receiver plane at the room and they are located at 8, 12 and 16 [m]. Based on the analysis in [9] and [39], the minimum illumination is set as $L_{min} = 0.05W/m^2$. The capacity gap from Shannon channel capacity is $\Upsilon = 0.35$. We assume that there are 20 timeslots during each frame. The traffic arrival of all the UEs follows Poisson distribution, and the mean traffic arrival rate is given by λ, where the specific value of λ will be given in each experiment. The traffic arrival rate and the RF channel conditions keep constant within one timeslot and changes on the timeslot boundaries (thus the small timescale network states). On the contrary, the UE locations keep constant within one frame and changes on the frame boundaries (thus the large timescale network states).

B. Convergence Speed

In the first experiment, we investigate the convergence speed of RF and VLC resource allocation algorithms. We observe from Fig. 4 that the proposed algorithm can converge fairly fast. Besides, the convergence speed is influenced by the Lyapunov term coefficient V. That is a larger V means a larger convergence speed. Fig. 5 shows the convergence speed of our proposed EAPC algorithm compared with the conventional approximated power control (APC) algorithm [34]. Specifically, the APC algorithm deals with the non-convex power control problem in (31) by directly applying the successive convex approximation and then solving the resultant convex approximation problems by the sub-gradient algorithm. It is shown in Fig. 5 that the EAPC algorithm requires only 4 to 6 iterations to find the optimal transmit power under different Lyapunov term coefficient V. Although there is a small improvement for the APC algorithm, it needs more iterations than the EAPC algorithm for realizing convergence, which is contradictory with our design motivation of time-efficient algorithm.

C. Dynamic Processes of ANRO Scheme

Fig. 6 depicts the instantaneous throughput of different APs under ANRO scheme. It is shown in Fig. 6(a) that the throughput of RF AP is changing dramatically along different frames. That is because the path loss model of RF AP is a function of UEs' locations, which is changing at the large timescale. Hence the throughput of RF AP is changing dramatically along different frames. While, at the small timescale, the throughput of the RF AP is changing within some certain range, which is resulted by the Gaussian random fast channel fading coefficients. Figs. 6(b)-(d) illustrate the throughput processes of VLC APs. We observe that the throughput of these APs are totally different during different frames, even more the throughput of these APs are zeros at some frames. That is because the unity frequency reuse across different VLC APs, the transmit powers of some VLC APs maybe cause severe interference to others. Therefore, these transmit powers will be controlled very small for maximizing the overall throughput. To sum up, Fig. 6 illustrates that our proposed ANRO scheme can adaptively handle the stochastic networks states and make the network stable.

Fig. 7(a) illustrates the instantaneous energy efficiency (EE) of RF AP, VLC APs and HetNet. In this experiment, the EE is defined as $\eta_{EE}(t) = \frac{\sum_{\tau=0}^{t-1}\mathbb{E}[R(\tau)]}{\sum_{\tau=0}^{t-1}\mathbb{E}[P(\tau)]}$. The figure shows that the VLC has very high EE due to the LEDs' low-power consumption and high achievable data rates. Moreover, it is obviously shown that the EE of HetNet is improved greatly by enabling the network with different technologies compared with the traditional homogeneous RF network. Therefore, the transmit power can be effectively reduced for transmitting the same amount of traffic data.

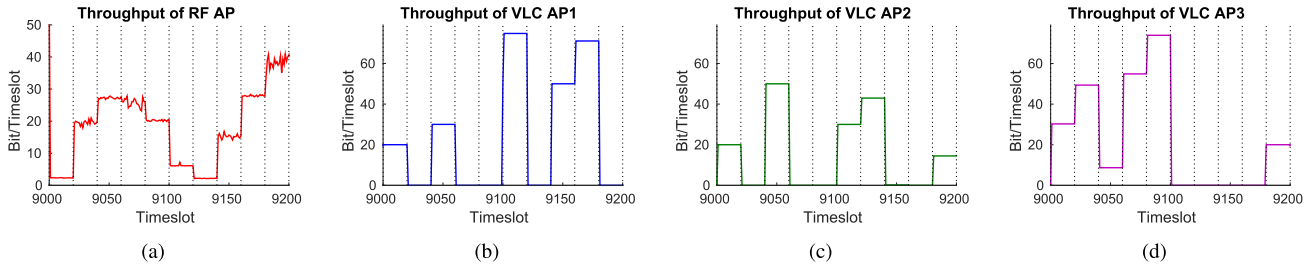

Fig. 6. Illustration of the throughputs on different APs.

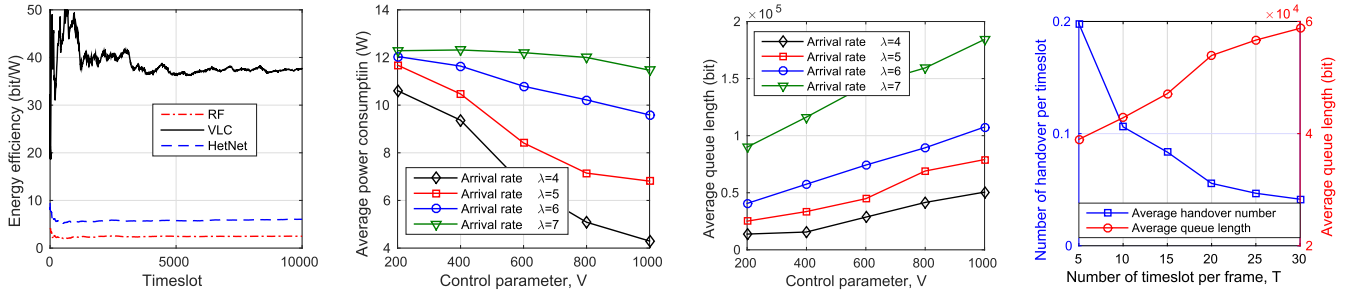

(a) Instantaneous energy efficiency of RF AP, VLC APs and HetNet.

(b) Time average power consumption versus control parameter V.

(c) Time average queue length versus control parameter V.

(d) Impact of parameter T on the system performance.

Fig. 7. Performance analysis of ANRO scheme.

D. Performance Tradeoff Under ANRO Scheme

In Figs. 7(b) and (c), we investigate the impacts of the control parameter V and the average traffic arrival rate λ on the tradeoff performance between the time average power consumption and the time average queue length. Fig. 7(b) shows the time average power consumption versus control parameter V. We notice that the power consumption decreases as V grows and that the larger the traffic arrival rate, the larger the power consumption. The reason can be found in Eq. (19). A larger V means that ANRO emphasizes more on power consumption and less on queue lengths. Fig. 7(c) shows the average queue length versus the control parameter V. We observe that the average queue length increases as V grows. As the traffic arrival rate increases, the average queue length also augments. Due to the fact that the average transmission delay is proportional to the average queue length from Littles Theorem [27], we can depict the average delay by the average queue length. Hence, our proposed algorithm achieves a tradeoff between time average power consumption and network delay. Therefore, we can obtain a significant rule for engineering design to flexibly balance the network power-delay performance. We only need to adjust appropriately the control parameter V to let the network operate in a predefined state.

In Fig. 7(d), we investigate the impact of parameter T, which is referred to as the number of timeslots in each frame, on the system performance. We assume that both connect and disconnect a link can incur network cost. Hence, the average handover number is defined as $\lim_{k\to\infty} \frac{1}{kT} \sum_{t=0}^{kT-1} ||\boldsymbol{\alpha}(t+1) - \boldsymbol{\alpha}(t)||_1$, where $||\cdot||_1$ is the l_1 norm. We observe that the average handover number decreases with the increase of T. This is the direct reaction of the increase of handover period T. However, with the increase of T, the average queue length increases. This is due to the fact that the queue lengths serve as weights in resource optimization problems (22)-(24) under our proposed ANRO scheme. At each timeslot, the ANRO can only obtain the queue lengths of this frame, i.e. $\mathbf{Q}(kT)$. The sensitivity of ANRO scheme to the queue lengths will decrease with the increase of parameter T, so that the average queue length increases. The figure shows that our proposed adaptive two-timescale resource optimization framework can effectively decrease the handover cost at a certain sacrifice of the queue length.

E. Performance Comparison

As the related work [40] do, in this experiment, we compare our proposed ANRO scheme with two benchmark schemes, i.e. RF-only and VLC-only. Specifically, RF-only scheme consists of a single RF wireless network at the location of 0 [m] and VLC-only scheme consists of three VLC APs, which are deployed at the same locations as ANRO scheme. To make it fair, we assume that all of these schemes have the same total maximum transmit power, i.e. 45W. In Figs. 8 (a) and (b), we illustrate the average queue length and the consumed average transmit power under different schemes against the number of UEs. From Fig. 8 (a), we observe that RF-only scheme obtains the smallest average queue length. However, it is shown in Fig. 8 (b) that RF-only scheme exhausts all of the transmit power. Fig. 8(b) also shows that VLC-only scheme achieves a smaller average transmit power than RF-only scheme, which reflects the energy efficiency of VLC APs. While, because the non-convex power

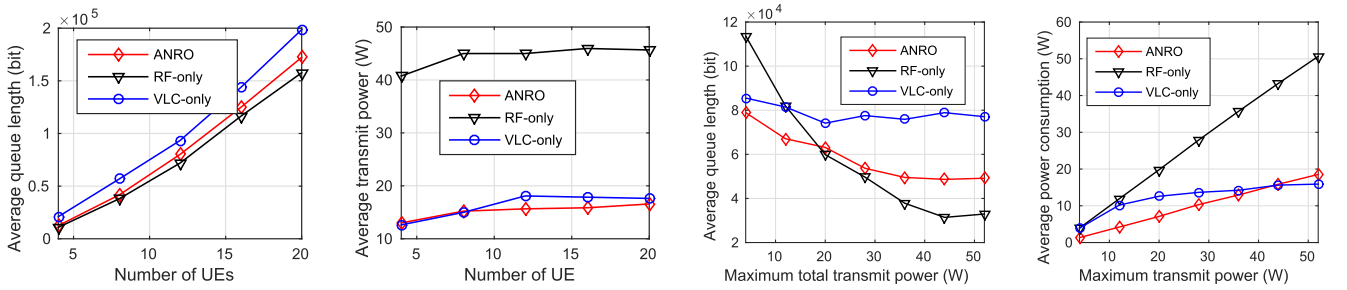

(a) Time average queue length against the number of UEs.

(b) Time average transmit power against the number of UEs.

(c) Time average queue length against maximum transmit power.

(d) Consumed average transmit power against maximum transmit power.

Fig. 8. Performance comparison between ANRO and other schemes.

control of the VLC APs, it cannot consume all of the transmit power to serve more UEs. By integrating of RF and VLC, our proposed ANRO scheme obtains the optimal average power consumption and a relative small average queue length. Therefore, these results demonstrate that the ANRO not only stabilizes the network but also significantly reduces the energy consumption than other existing schemes.

Figs. 8(c) and (d) show the average queue length and the consumed average transmit power under different schemes against the maximum allowed transmit power. We observe that when the maximum allowed transmit power is small, ANRO scheme not only achieves the smallest average queue length but also consumes the minimum transmit power. With the increase of the maximum allowed transmit power, RF-only scheme obtains the smallest average queue length. However, we observe from Fig. 8(d) that RF-only scheme greedily exhausts all of the maximum allowed transmit power. Fig. 8(c) shows that VLC-only scheme results the largest average queue length. That is because the mutual interference among VLC APs results in a nonconvex SINR, too large transmit power of one VLC AP will cause severe interference to others, so that it cannot provide more throughput with the increase of the maximum allowed transmit power. However, in ANRO scheme, these extra transmit power can be transferred from the VLC APs to the RF AP, so that ANRO can stabilize the network, whilst minimizing the transmit power.

VII. Conclusion

In this paper, we considered the adaptive network resource optimization for a HetNet combining with RF and VLCs. An online two-timescale ANRO framework was proposed for adapting to the stochastic traffic arrival rates and dynamic wireless channel conditions. In ANRO, the network selections for UEs and as well the joint transmission scheduling and power control for VLC APs were operated at the large timescale, while the resource allocation for RF AP was operated at the small timescale. Then, we developed corresponding easy-to-realize strategies for the two timescale resource optimizations. Finally, we showed that the ANRO can achieve a tradeoff between network power consumption and delay. Furthermore, it not only can stabilize the network but also can significantly reduce the energy consumption compared with other existing schemes.

References

[1] L. Hanzo, H. Haas, S. Imre, D. O'Brien, M. Rupp, and L. Gyongyosi, "Wireless myths, realities, and futures: From 3G/4G to optical and quantum wireless," *Proc. IEEE*, vol. 100, Special Centennial Issue, pp. 1853–1888, May 2012.

[2] M. Ayyash *et al.*, "Coexistence of WiFi and LiFi toward 5G: Concepts, opportunities, and challenges," *IEEE Commun. Mag.*, vol. 54, no. 2, pp. 64–71, Feb. 2016.

[3] H. Ju, B. Liang, J. Li, Y. Long, and X. Yang, "Adaptive cross-network cross-layer design in heterogeneous wireless networks," *IEEE Trans. Wireless Commun.*, vol. 14, no. 2, pp. 655–669, Feb. 2015.

[4] S. Hayashi and Z.-Q. Luo, "Spectrum management for interference-limited multiuser communication systems," *IEEE Trans. Inf. Theory*, vol. 55, no. 3, pp. 1153–1175, Mar. 2009.

[5] W. Wu, F. Zhou, and Q. Yang, "Dynamic network resource optimization in hybrid VLC and radio frequency networks," in *Proc. MoWNeT*, May 2017, pp. 1–7.

[6] H. Yu, M. H. Cheung, L. Huang, and J. Huang, "Power-delay tradeoff with predictive scheduling in integrated cellular and Wi-Fi networks," *IEEE J. Sel. Areas Commun.*, vol. 34, no. 4, pp. 735–742, Apr. 2016.

[7] P. H. Pathak, X. Feng, P. Hu, and P. Mohapatra, "Visible light communication, networking, and sensing: A survey, potential and challenges," *IEEE Commun. Surveys Tuts.*, vol. 17, no. 4, pp. 2047–2077, 4th Quart., 2015.

[8] X. Li, F. Jin, R. Zhang, J. Wang, Z. Xu, and L. Hanzo, "Users first: User-centric cluster formation for interference-mitigation in visible-light networks," *IEEE Trans. Wireless Commun.*, vol. 15, no. 1, pp. 39–53, Jan. 2016.

[9] R. Zhang, H. Claussen, H. Haas, and L. Hanzo, "Energy efficient visible light communications relying on amorphous cells," *IEEE J. Sel. Areas Commun.*, vol. 34, no. 2, pp. 894–906, Apr. 2016.

[10] J. M. Kahn and J. R. Barry, "Wireless infrared communications," *Proc. IEEE*, vol. 85, no. 2, pp. 265–298, Feb. 1997.

[11] J. Jiang *et al.*, "Video streaming in the multiuser indoor visible light downlink," *IEEE Access*, vol. 3, pp. 2959–2986, 2015.

[12] S. Shao *et al.*, "Design and analysis of a visible-light-communication enhanced WiFi system," *IEEE/OSA J. Opt. Commun. Netw.*, vol. 7, no. 10, pp. 960–973, Oct. 2015.

[13] M. B. Rahaim *et al.*, "A hybrid radio frequency and broadcast visible light communication system," in *Proc. IEEE GLOBECOM Workshops (GC Wkshps)*, Dec. 2011, pp. 792–796.

[14] X. Li, R. Zhang, and L. Hanzo, "Cooperative load balancing in hybrid visible light communications and WiFi," *IEEE Trans. Commun.*, vol. 63, no. 4, pp. 1319–1329, Apr. 2015.

[15] D. A. Basnayaka and H. Haas, "Hybrid RF and VLC systems: Improving user data rate performance of VLC systems," in *Proc. IEEE 81st Veh. Technol. Conf. (VTC Spring)*, Scotland, U.K., May 2015, pp. 1–5.

[16] F. Jin, R. Zhang, and L. Hanzo, "Resource allocation under delay-guarantee constraints for heterogeneous visible-light and RF femtocell," *IEEE Trans. Wireless Commun.*, vol. 14, no. 2, pp. 1020–1034, Feb. 2015.

[17] F. Jin, X. Li, R. Zhang, C. Dong, and L. Hanzo, "Resource allocation under delay-guarantee constraints for visible-light communication," *IEEE Access*, vol. 4, pp. 7301–7312, 2016.

[18] Y. Wang and H. Haas, "Dynamic load balancing with handover in hybrid Li-Fi and Wi-Fi networks," *J. Lightw. Technol.*, vol. 33, no. 22, pp. 4671–4682, Nov. 15, 2015.
[19] S. Shao and A. Khreishah, "Delay analysis of unsaturated heterogeneous omnidirectional-directional small cell wireless networks: The case of RF-VLC coexistence," *IEEE Trans. Wireless Commun.*, vol. 15, no. 12, pp. 8406–8421, Dec. 2016.
[20] S. Shao, A. Khreishah, and M. Ayyash. (2015). "Delay analysis of hybrid WiFi-LiFi system." [Online]. Available: https://arxiv.org/abs/1510.00740
[21] J. Chen and V. K. N. Lau. (2013). "Convergence analysis of mixed timescale cross-layer stochastic optimization." [Online]. Available: https://arxiv.org/abs/1305.0153
[22] H. Jung, T. T. Kwon, K. Cho, and Y. Choi, "React: Rate adaptation using coherence time in 802.11 WLANs," *Comput. Commun.*, vol. 34, no. 11, pp. 1316–1327, 2011.
[23] A.-L. Chen, H.-P. Wu, Y.-L. Wei, and H.-M. Tsai, "Time variation in vehicle-to-vehicle visible light communication channels," in *Proc. IEEE Veh. Netw. Conf. (VNC)*, Dec. 2016, pp. 1–8.
[24] S. Dimitrov, S. Sinanovic, and H. Haas, "Clipping noise in OFDM-based optical wireless communication systems," *IEEE Trans. Commun.*, vol. 60, no. 4, pp. 1072–1081, Apr. 2012.
[25] D. Bethanabhotla, G. Caire, and M. J. Neely, "Adaptive video streaming for wireless networks with multiple users and helpers," *IEEE Trans. Commun.*, vol. 63, no. 1, pp. 268–285, Jan. 2015.
[26] L. Georgiadis, M. J. Neely, and L. Tassiulas, "Resource allocation and cross-layer control in wireless networks," *Found. Trends Netw.*, vol. 1, no. 1, pp. 1–144, 2006.
[27] D. P. Bertsekas and R. G. Gallager, *Data Networks*. Englewood Cliffs, NJ, USA: Prentice-Hall, 1987.
[28] F. Fu and M. van der Schaar, "A systematic framework for dynamically optimizing multi-user wireless video transmission," *IEEE J. Sel. Areas Commun.*, vol. 28, no. 3, pp. 308–320, Apr. 2010.
[29] Y. Cui, V. K. N. Lau, R. Wang, H. Huang, and S. Zhang, "A survey on delay-aware resource control for wireless systems—Large deviation theory, stochastic Lyapunov drift, and distributed stochastic learning," *IEEE Trans. Inf. Theory*, vol. 58, no. 3, pp. 1677–1701, Mar. 2012.
[30] M. J. Neely, *Stochastic Network Optimization With Application to Communication and Queueing Systems*. San Rafael, CA, USA: Morgan & Claypool, 2010.
[31] M. U. Farooq, Khubaib, and L. K. John, "Store-load-branch (SLB) predictor: A compiler assisted branch prediction for data dependent branches," in *Proc. IEEE 19th Int. Symp. High Perform. Comput. Archit. (HPCA)*, Feb. 2013, pp. 59–70.
[32] M. K. Ozdemir and H. Arslan, "Channel estimation for wireless OFDM systems," *IEEE Commun. Surveys Tuts.*, vol. 9, no. 2, pp. 18–48, 2nd Quart., 2007.
[33] L. Huang, S. Zhang, M. Chen, and X. Liu, "When backpressure meets predictive scheduling," *IEEE/ACM Trans. Netw.*, vol. 24, no. 4, pp. 2237–2250, Aug. 2016.
[34] Q. Chen, G. Yu, R. Yin, and G. Y. Li, "Energy-efficient user association and resource allocation for multistream carrier aggregation," *IEEE Trans. Veh. Technol.*, vol. 65, no. 8, pp. 6366–6376, Aug. 2016.
[35] S. Parsaeefard, R. Dawadi, M. Derakhshani, and T. Le-Ngoc, "Joint user-association and resource-allocation in virtualized wireless networks," *IEEE Access*, vol. 4, pp. 2738–2750, 2016.
[36] C. Guo, B. Liao, L. Huang, P. Zhang, M. Huang, and J. Zhang, "On proportional fairness in power allocation for two-tone spectrum-sharing networks," *IEEE Trans. Veh. Technol.*, vol. 65, no. 12, pp. 10090–10096, Dec. 2016.
[37] N. Mokari, M. R. Javan, and K. Navaie, "Cross-layer resource allocation in OFDMA systems for heterogeneous traffic with imperfect CSI," *IEEE Trans. Veh. Technol.*, vol. 59, no. 2, pp. 1011–1017, Feb. 2010.
[38] J. Li, M. Peng, Y. Yu, and Z. Ding, "Energy-efficient joint congestion control and resource optimization in heterogeneous cloud radio access networks," *IEEE Trans. Veh. Technol.*, vol. 65, no. 12, pp. 9873–9887, Dec. 2016.
[39] J. Grubor, S. Randel, K.-D. Langer, and J. Walewski, "Broadband information broadcasting using LED-based interior lighting," *J. Lightw. Technol.*, vol. 26, no. 24, pp. 3883–3892, Dec. 15, 2008.
[40] M. Kashef, M. Ismail, M. Abdallah, K. A. Qaraqe, and E. Serpedin, "Energy efficient resource allocation for mixed RF/VLC heterogeneous wireless networks," *IEEE J. Sel. Areas Commun.*, vol. 34, no. 4, pp. 883–893, Apr. 2016.

Weihua Wu received the B.S. and M.E. degrees in telecommunications engineering and the Ph.D. degree in communication and information systems from Xidian University, China, in 2011, 2014, and 2017, respectively. From 2016 to 2017, he was a Visiting Student with the University of Avignon. Since 2018, he has been with the School of Telecommunications Engineering, Xidian University, where he is currently an Assistant Professor. His research interests include wireless resource allocation and stochastic network optimization and their applications in multihoming wireless networks.

Fen Zhou (M'15–SM'16) received the Ph.D. degree in networking from INSA Rennes in 2010. He held a post-doctoral position at Telecom Bretagne, for two years. He has been an Associate Professor with the LIA Laboratory, University of Avignon, France, since 2012. He is currently with the LISITE Laboratory, Institut Supérieur d'Electronique de Paris, France. His research interests include routing and resource allocation in networking (with a focus on optical networks) and routing optimization in intelligent transportation systems. He has served as the Symposium Co-Chair, the Publicity Co-Chair, the Local Organization Chair, and the Session Chair in several international conferences, such as the IEEE ICNC18, IEEE WCSP14, IEEE Wimob15, NetgCOOP16, IEEE MovNet17, and IEEE Globecom13. He has also served on the program committees for several international conferences such as INFOCOM, ICC, GLOBECOM, and ONDM.

Qinghai Yang received the B.S. degree in communication engineering from the Shandong University of Technology, China, in 1998, the M.S. degree in information and communication systems from Xidian University, China, in 2001, and the Ph.D. degree in communication engineering from Inha University, South Korea, in 2007. From 2007 to 2008, he was a Research Fellow at UWB-ITRC, South Korea. Since 2008, he has been with Xidian University, China. His current research interest include the fields of autonomic communication, content delivery networks, and LTE-A techniques. He received the University-President Award.